
05 Sep 2020

Component Analysis of Bio-Asphalt Binder Using Crumb Rubber Modifier and Guayule Resin as an Innovative Asphalt Replacer

Ahmed Hemida

Magdy Abdelrahman

Missouri University of Science and Technology, abdelrahmanm@mst.edu

Follow this and additional works at: https://scholarsmine.mst.edu/civarc_enveng_facwork



Part of the [Structural Engineering Commons](#)

Recommended Citation

A. Hemida and M. Abdelrahman, "Component Analysis of Bio-Asphalt Binder Using Crumb Rubber Modifier and Guayule Resin as an Innovative Asphalt Replacer," *Preprints*, Sep 2020.



This work is licensed under a [Creative Commons Attribution 4.0 License](#).

This Article - Preprint is brought to you for free and open access by Scholars' Mine. It has been accepted for inclusion in Civil, Architectural and Environmental Engineering Faculty Research & Creative Works by an authorized administrator of Scholars' Mine. This work is protected by U. S. Copyright Law. Unauthorized use including reproduction for redistribution requires the permission of the copyright holder. For more information, please contact scholarsmine@mst.edu.

1 Component analysis of bio-asphalt binder using crumb rubber 2 modifier and guayule resin as an innovative asphalt replacer

3 Ahmed Hemida ^{a,*}, Magdy Abdelrahman ^b

4 ^a Ph.D. Candidate, Department of Civil, Architectural, and Environmental Engineering, Missouri University of
5 Science and Technology (Missouri S&T), Rolla, MO 65409, USA

6 ^b Missouri Asphalt Pavement Association (MAPA) Endowed Professor, Department of Civil, Architectural,
7 and Environmental Engineering, Missouri University of Science and Technology (Missouri S&T), Rolla, MO
8 65409, USA

9 * Corresponding author.

10 E-mail addresses: amhbnc@mst.edu (A. Hemida), m.abdelrahman@mst.edu (M. Abdelrahman).

11 ABSTRACT

12 This research seeks to interpret the component analysis of an innovative bio-asphalt binder using guayule resin
13 in addition to crumb rubber modifier (CRM) at high concentrations. Such asphalt modification aims to minimize
14 the dependency on virgin asphalt binder and provide new solutions concerning sustainable, flexible pavement
15 industry. Guayule resin is a promising bioresource for asphalt binder replacement. By now, it could be
16 considered a no value byproduct extracted during the guayule natural rubber production. CRM is a recycled
17 material derived from scrap tires. The provided interpretation could help in understanding the asphalt-rubber-
18 guayule interaction mechanism. Fourier transform infrared spectroscopy (FTIR), supported by thermo-
19 gravimetric analysis (TGA), was used to investigate the component analyses of guayule resin composition,
20 asphalt guayule interaction, and asphalt rubber guayule interaction, compared to corresponding asphalt rubber
21 interaction. Additionally, the rheological properties at elevated temperatures were provided to link the
22 microscale properties with the final product performance. The study clarified the distinct carbon and hydrogen
23 compositional elements of guayule resin. Asphalt and guayule resin have similarities in chemical composition
24 and rheological behavior with temperature susceptibility. The asphalt guayule binder had physical interaction.
25 However, when both interacted with rubber, a chemical interaction was attributed, with no difference in rubber
26 dissolution tendency, in asphalt rubber guayule, compared to asphalt rubber. A bio-binder composed of 62.5%
27 asphalt, 25% guayule and 12.5% CRM had the potential to provide rheological properties better than base
28 asphalt. Such behavior was interpreted by a high release of rubber components.

29 **Keywords:** Asphalt rubber; Bio-binder; Component analysis; FTIR; Guayule resin; TGA.

30 1. Introduction

31 Guayule resin is inevitably extracted as a bio-based by-product during the guayule natural rubber
32 (intentionally main guayule shrub derivative) production (Nakayama, 2005). Guayule resin represents $\pm 10\%$ of
33 the total dry biomass (Rasutis et al., 2015), whereas guayule rubber represents almost the same concentration
34 (Hemida and Abdelrahman, 2018). In addition, other derivatives are extracted from guayule shrub, such as
35 bagasse ($\pm 80\%$ of total dry biomass) (Rasutis et al., 2015; Schloman Jr et al., 1986). Guayule commercialization
36 deserves future research investigations since they may enhance the guayule shrub sustainability in terms of
37 economic and environmental concerns (Rasutis et al., 2015). Literature showed that guayule natural rubber is
38 significantly competitive to the current global source of natural rubber (Hevea) (Rasutis et al., 2015). Guayule
39 rubber is a potential domestic natural rubber source of the USA, which could be national security against the

40 domination of natural rubber production by Southeast Asia (over 90% of the global natural rubber production)
41 (Rasutis et al., 2015). The major restriction that most likely stands against the guayule natural rubber production
42 is the economic factors, which could be balanced by getting advantage of other derivatives (bio-based by-
43 products) (Rasutis et al., 2015).

44 Guayule resin seems an asphalt-like material: viscoelastic and temperature susceptible (Hemida and
45 Abdelrahman, 2018, 2019a, 2020a, b). However, since the flexible pavement binder is required to have specific
46 grades in order to accomplish the required characterization, the guayule resin as a bioresource may not be
47 desired alone. Hemida and Abdelrahman (Hemida and Abdelrahman, 2018, 2019a, 2020a, b) have previously
48 investigated the influence of adding guayule resin as an asphalt replacer on the asphalt rubber (AR). Guayule
49 resin could provide a benefit as a bio-based by-product; potentially economic, renewable, and environmentally
50 friendly, unlike asphalt cement (Hemida and Abdelrahman, 2018, 2019a, 2020a, b). It has potential to be utilized
51 in the massive flexible pavement industry (Hemida and Abdelrahman, 2018, 2019a). Overall, bio-binders could
52 provide new solutions in terms of sustainability, economics, and environmental concerns (Hemida and
53 Abdelrahman, 2018, 2019a, b). Chemical analysis of the AR has been studied in the literature to a high extent
54 (Nivitha et al., 2016; Ragab, 2016; Ragab and Abdelrahman, 2018; Ragab et al., 2013b). The authors in this
55 study are looking forward to partially replacing AR by 25–75% guayule resin for sustainable, flexible pavement
56 (Hemida and Abdelrahman, 2019a, 2020a). Asphalt, rubber, and asphalt rubber interaction could help
57 understand the contribution of such a replacer on the final modified asphalt since they have been covered in
58 literature.

59 The literature clarified that the base asphalt had symmetric and asymmetric C–H stretches in CH₂ and CH₃
60 at wavenumbers in a range of 3000–2800 cm⁻¹ (Nivitha et al., 2016). It involved four distinct peaks in this range
61 (around 2954 cm⁻¹ (Ragab, 2016; Socrates, 2004), 2924 cm⁻¹ (Ragab, 2016; Zhang et al., 2009), 2870 cm⁻¹
62 (Ragab, 2016; Socrates, 2004; TFS, 2019), and 2853 cm⁻¹ (Ragab, 2016; Yao et al., 2013; Zhang et al., 2009)).
63 Other peaks were formed around 1458 cm⁻¹ (Ragab, 2016; Yao et al., 2013; Zhang et al., 2009) and 1376 cm⁻¹
64 (Ragab, 2016; Yao et al., 2013; Zhang et al., 2011) for the same functional group, indicating symmetric and
65 asymmetric bends of CH₃ (Bassler, 1981; Smith, 1998). Such functional groups were compatible with the
66 elemental composition of base asphalt (around 80% carbon and 10% hydrogen) (Nivitha et al., 2016). Other
67 distinct peaks were observed at 1730 cm⁻¹ and 1032 cm⁻¹ for C=O (Ragab, 2016; Yao et al., 2013; Zhang et al.,
68 2009) and S=O (Masson et al., 2001; Ragab, 2016; Zhang et al., 2011), respectively. Likewise, the aromatic
69 peak was associated with C=C at 1603 cm⁻¹ (Ragab, 2016; Yao et al., 2013; Zhang et al., 2011). Four carbon
70 atoms in a row were observed at 721 cm⁻¹ (Nivitha et al., 2016).

71 The CRM is composed of rubber/elastomers, carbon black, metallic components, and other additives. Their
72 proportions differ according to the tire type (car, truck/bus, or mix) (Presti, 2013). In other words, the CRM
73 includes natural rubber (cis-isoprene, mainly responsible for elasticity), synthetic rubber (styrene-butadiene
74 rubber [SBR], mainly responsible for thermal stability), metallic elements (containing 15–20% polar
75 components, highly reactive), and carbon black and textiles (organic fillers) (Nivitha et al., 2016). Though the
76 primary asphalt rubber interaction was physical, the chemical interaction could take place (Nivitha et al., 2016).
77 Normally, it needs higher interaction temperatures to be observed (170–200°C) since the devulcanization and/or
78 depolymerization may occur causing a rubber dissolution in asphalt (Zanzotto and Kennepohl, 1996). It was
79 rarely seen at lower than this range of interaction temperatures (Nivitha et al., 2016). In literature, the gel
80 permeation chromatography (GPC) showed a reduction in chain length of rubber when interacted with asphalt,
81 indicating its depolymerization in the internal asphalt structure (Billiter et al., 1997; Chipps et al., 2001). In
82 terms of Fourier transform infrared spectroscopy (FTIR) analysis of CRM, the literature claimed that four strong
83 sharp peaks were created for N–H stretches between 3500–3000 cm⁻¹ corresponding to amines involved in
84 CRM. The NH₂ asymmetric stretch was formed in a wavenumber range of 3500–3420 cm⁻¹. The peak of NH₂
85 symmetric stretch could be found in a wavenumber range of 3500–3420 cm⁻¹. The peak of NH₂ scissors stretch
86 could be found at 1637 and 1616 cm⁻¹. Aromatic secondary amine could be formed at 3414 cm⁻¹, and saturated
87 secondary amine or amide could be found at 3238 cm⁻¹ (Nivitha et al., 2016). On the other hand, the
88 concentration of sulfur in CRM was about 1–2% depending on the tire type (car or truck/bus) (Presti, 2013;
89 Thodesen et al., 2009). Sulfur in CRM could be attributed to either C–S or S–S functional groups (Nivitha et

90 al., 2016). Since the absorbance of N–H stretch in CRM was significantly high, it was not easy to identify the
91 sulfur bonds as their absorbance was very low in a range of 500–700 cm^{-1} . Likewise, CRM contained aliphatic
92 C–H stretch in the region of 3000–2800 cm^{-1} , which had short peaks for the last-mentioned reason. The SBR
93 peak was created at 965 cm^{-1} , indicating =C–H in phase out-of-plane bending of trans-1,4-butadiene, and
94 masked by N–H scissoring vibration as reported by Nivitha et al. (Nivitha et al., 2016).

95 Nivitha et al. (Nivitha et al., 2016) investigated the crumb rubber modified asphalt (CRMA) using FTIR,
96 concluding a similarly formed spectrum for both base asphalt and CRMA, except for a few distinct peaks. Only
97 one amine peak was observed at 3300 cm^{-1} , indicating secondary amine/amide. With heating to more than
98 100°C, amines reacted with carboxylic acid yielding ammonium carboxylate salt, losing water molecule to
99 produce a secondary amide. Accordingly, it was expected that this could also occur as carboxylic acid was
100 present in asphalt. The SBR peak was formed at 965 cm^{-1} in CRMA, similar to its formation in CRM (i.e., no
101 observed peak shift) (Nivitha et al., 2016).

102 In previous work by Hemida and Abdelrahman (Hemida and Abdelrahman, 2019a), a partial asphalt
103 replacement was applied to utilize guayule resin. The CRM was used to compensate for the performance
104 decrease by adding guayule resin to the base asphalt, triggering the same base asphalt performance, at the very
105 least. The CRM was proven to be an asphalt enhancer (Ragab, 2016). In this regard, the literature addressed
106 such enhancement based on interaction parameters (time, temperature, and speed) and material parameters
107 (asphalt grade and CRM source and size). Interaction temperature could be the major parameter influencing the
108 dissolution of CRM into the liquid asphalt (Ghavibazoo et al., 2013b; Ragab et al., 2013a). Researchers have
109 proven that a 190°C interaction temperature and a 3000 rpm interaction speed could provide the most enhanced
110 CRMA (Ghavibazoo et al., 2013b; Ragab et al., 2013a). Because of the cross-linked structure of CRM, it is not
111 easy to entirely dissolve in the liquid binder (Zanzotto and Kennepohl, 1996). However, the three-dimension
112 network structure was associated with the CRMA at the recommended interaction parameters above (Ragab et
113 al., 2013b). Three-dimension networking was proven to enhance the binder rheological properties (Ragab et al.,
114 2013b). Therefore, following the literature, the recommended interaction parameters could be a good initiative
115 to apply with the innovative asphalt-rubber-guayule binder (also called bio-binder in this study).

116 This research mainly seeks to interpret the component analysis of an innovative bio-binder made of guayule
117 resin (promising bioresource for asphalt binder replacement) and crumb rubber modifier. This interpretation
118 will help in understanding the asphalt rubber guayule interaction mechanism. In other words, the authors in this
119 study seek to explore the applicability of using guayule resin as an innovative asphalt replacer from the
120 engineering viewpoint. It is believed that researchers can enhance such an innovative bio-binder in the future
121 based on conceptual research. Literature covered asphalt rubber interaction in a satisfying manner. However,
122 guayule resin still needs to be chemically understood to investigate its chemical influence on asphalt rubber.
123 Accordingly, this paper provides an attempt to analyze such an innovative bio-binder by FTIR analysis of the
124 designated liquid bio-binders, verified by FTIR analysis of extracted CRM from such bio-binders, and
125 supported by some TGA analysis. Additionally, the rheological properties at elevated temperatures were
126 provided to link the microscale properties with the final product performance (Hemida and Abdelrahman,
127 2019a).

128 **2. Materials and Methods**

129 **2.1. Materials**

130 In this research, a selection of five designated asphalt rubber guayule (AR-BGR) bio-binders was
131 established after multiple attempts of different concentrations of AC, guayule resin made by Bridgestone
132 (BGR), and CRM, as listed in **Table 1**. The sources of AC, BGR, and CRM were Philips 66 Company, IL;
133 Bridgestone Corp; and Liberty Tire Recycling, respectively. CRM 30–40 (passed mesh #30 and retained on
134 mesh #40) was used in this study based on the US standard system (Ghavibazoo et al., 2013a; Zauamanis et al.,

135 2014). In order to evaluate the impact of guayule resin, such designated bio-binders were compared to ARs by
136 adding extra AC instead of BGR, same concentration.

137 The binder codes contained two parts (left and right). The left part was either AR-BGR or AR, and the right
138 part was 25-10, 50-15, 50-20, 75-10, or 75-20. For instance, AR-BGR25-10 denoted 25% of AR (comprising
139 10% of CRM by wt. of AC) and 75% of BGR. AR25-10 denoted its corresponding AR (i.e., AC replaced the
140 BGR portion). Ultimately, either AR-BGR bio-binder or its corresponding AR binder involved the same CRM
141 concentration in the overall blend. Likewise, binders were designated as WMs and LPs. When relevant, “WM”
142 was enclosed to the binder code (e.g., AR-BGR25-10WM), as was “LP” (e.g., AR-BGR25-10LP).

143 The blends were created using a high shear mixer with an accurate heating assembly of a heating mantle
144 and a temperature controller. As a part of the preparation process, the as-received guayule resin (coded G) was
145 stirred at 160°C for 4 hr with 600 rpm to make sure that no moisture or low molecular weight components were
146 involved (coded G4), as verified in a previous study (Hemida and Abdelrahman, 2019a). The AC was mixed
147 with CRM for 40 min at 190°C and 3000 rpm. The G4 was added by decreasing the temperature and speed to
148 160°C and 600 rpm, respectively, for 1 hr. For ARs, extra AC was added to the initial asphalt rubber blend,
149 instead of guayule resin, following the same interaction parameters.

150 **Table 1. Binder designation and properties.**

Binder	Binder Code	CRM%	CRM%	AC	AR	BGR	WM		LP	
		by wt. of AC		by wt. of blend			Pass/Fail Temp [°C]	PG	Pass/Fail Temp [°C]	PG
Base asphalt	AC						66	64	66	64
As-received guayule	G						55	52	55	52
4-hr Heat-Treated BGR	G4						57	52	57	52
25%(AR10%)+75%BGR	AR-BGR25-10	10	2.3	22.7	25	75	59	58	59	58
25%(AR10%)+75%AC	AR25-10	2.4	2.3	97.7	100		68	64	67	64
50%(AR15%)+50%BGR	AR-BGR50-15	15	6.5	43.5	50	50	64	64	62	58
50%(AR15%)+50%AC	AR50-15	7	6.5	93.5	100		72	70	69	64
50%(AR20%)+50%BGR	AR-BGR50-20	20	8.3	41.7	50	50	65	64	62	58
50%(AR20%)+50%AC	AR50-20	9.1	8.3	91.7	100		74	70	70	70
75%(AR10%)+25%BGR	AR-BGR75-10	10	6.8	68.2	75	25	67	64	65	64
75%(AR10%)+25%AC	AR75-10	7.3	6.8	93.2	100		73	70	70	64
75%(AR20%)+25%BGR	AR-BGR75-20	20	12.5	62.5	75	25	72	70	68	64
75%(AR20%)+25%AC	AR75-20	14.3	12.5	87.5	100		80	76	74	70

151

152 2.2. Methods

153 2.2.1. Extracted liquid phase and crumb rubber modifier

154 In order to study the chemical analysis of AR-BGRs and corresponding ARs by FTIR, the liquid binder was
155 acquired. Mesh #200 was used to extract the liquid binder at 165°C for about 25 min. The extracted liquid binder was
156 kept in a freezer at -12°C to ensure no undesired reaction or aging (Daly et al., 2010; Ghavibazoo and Abdelrahman,
157 2014; Ghavibazoo et al., 2013a).

158 In order to study the reduction of the dispersed CRM particle radius and the CRM composition analysis by the
159 FTIR, the CRM (particle) residue was extracted. CRM was extracted by dissolving a sample of 10 ± 2 g of the binder
160 whole matrix in a 100 gram of trichloroethylene. The solution was filtrated in a mesh #200 to retain the CRM particle
161 residue and washed by extra clean TCE until it became colorless. The extracted CRM was placed in an oven at 60°C
162 to ensure no TCE remaining. A similar dissolution method was applied in literature (Daly et al., 2010; Ghavibazoo
163 and Abdelrahman, 2014; Ghavibazoo et al., 2013a, b) on AR. Likewise, Hemida and Abdelrahman (Hemida and
164 Abdelrahman, 2019a) proved almost 100% solubility of guayule resin in TCE.

165 2.2.2. *Dynamic shear rheometer*

166 In terms of Superpave grading system, the high-temperature grade and pass/fail temperature were measured using
 167 Anton Paar DSR (MCR302). A gap of 2 mm was utilized for all CRM-involved binders (Diab and You, 2017; Lee et
 168 al., 2008; Shen and Amirkhanian, 2005). Otherwise, a gap of 1 mm was used for all liquid binders (AASHTO, 2013).
 169 AASHTO T315 was followed for all rheological tests (AASHTO, 2013).

170 2.2.3. *FTIR*

171 The Nicolet iS50 FTIR was used to study the chemical analysis of guayule resin, original CRM, extracted CRM
 172 from AR-BGRs, and their corresponding ARs (same CRM concentration and same interaction parameters), in addition
 173 to the liquid binders extracted from AR-BGRs and ARs. In literature, some researchers used the KBr disks to
 174 investigate the modified asphalt samples. However, this method requires a dilution of modified asphalt samples by a
 175 solvent such as toluene to get a thin film layer formed between two KPr disks to facilitate the infrared beam in order
 176 to penetrate the specimen and detect the functional groups represented by formed peaks at specific wavenumbers
 177 (Glaser et al., 2013; Huang et al., 2012; Ragab, 2016). Furthermore, this method affects the original internal structure
 178 properties of the modified asphalt. Accordingly, the authors in this research used a method that directly dealt with the
 179 original sample (without any solvent interference). This technique was implemented using an FTIR spectrometer
 180 equipped with a diamond attenuated total reflection (ATR) sample cell (FTIR-ATR) (Diab and You, 2017). Overall,
 181 the FTIR was used by many researchers to investigate CRMA and polymer modified asphalt (PMA) in order to show
 182 the solubility (or dissolution) of polymer/rubber components in the liquid binder of the modified asphalt (Deef-Allah
 183 et al., 2020; Masson et al., 2001; Nivitha et al., 2016; Zhang et al., 2011). For example, peaks at 966 to 969 cm⁻¹ and
 184 1600 cm⁻¹ were distinct for styrene butadiene styrene (SBS) or styrene-ethylene butadiene styrene (SEBS) (Ragab,
 185 2016).

186 2.2.4. *TGA*

187 TGA is the most common thermal analysis technique. Many researchers have used the TGA instrument to analyze
 188 the multi-component samples since each component has its decomposition temperature (Deef-Allah et al., 2020;
 189 Ragab, 2016; Ragab and Abdelrahman, 2018; Ragab et al., 2013a). A modifier such as CRM could be analyzed by
 190 the ramp (conventional) method, as its components are relatively away from each other. It is easy to distinguish them
 191 with the ramp method limitations. In this research, the ramp method using TA Q50 TGA was utilized to investigate
 192 the CRM dissolution, either original or extracted out of the liquid bio-binder. The literature interpreted the
 193 decomposition temperature ranges of CRM components (Hemida and Abdelrahman, 2020b; Ragab, 2016; Ragab et
 194 al., 2013a), and divided the CRM decomposition into four regions:

- 195 1) 25 to 300°C for oily components,
- 196 2) 300°C to the temperature at the lowest point on the derivative thermo-gravimetric (DTG) curve for natural
 197 rubber,
- 198 3) the end of second region to 500°C for synthetic rubber, and
- 199 4) the residue at 500°C for filler components (e.g., carbon black).

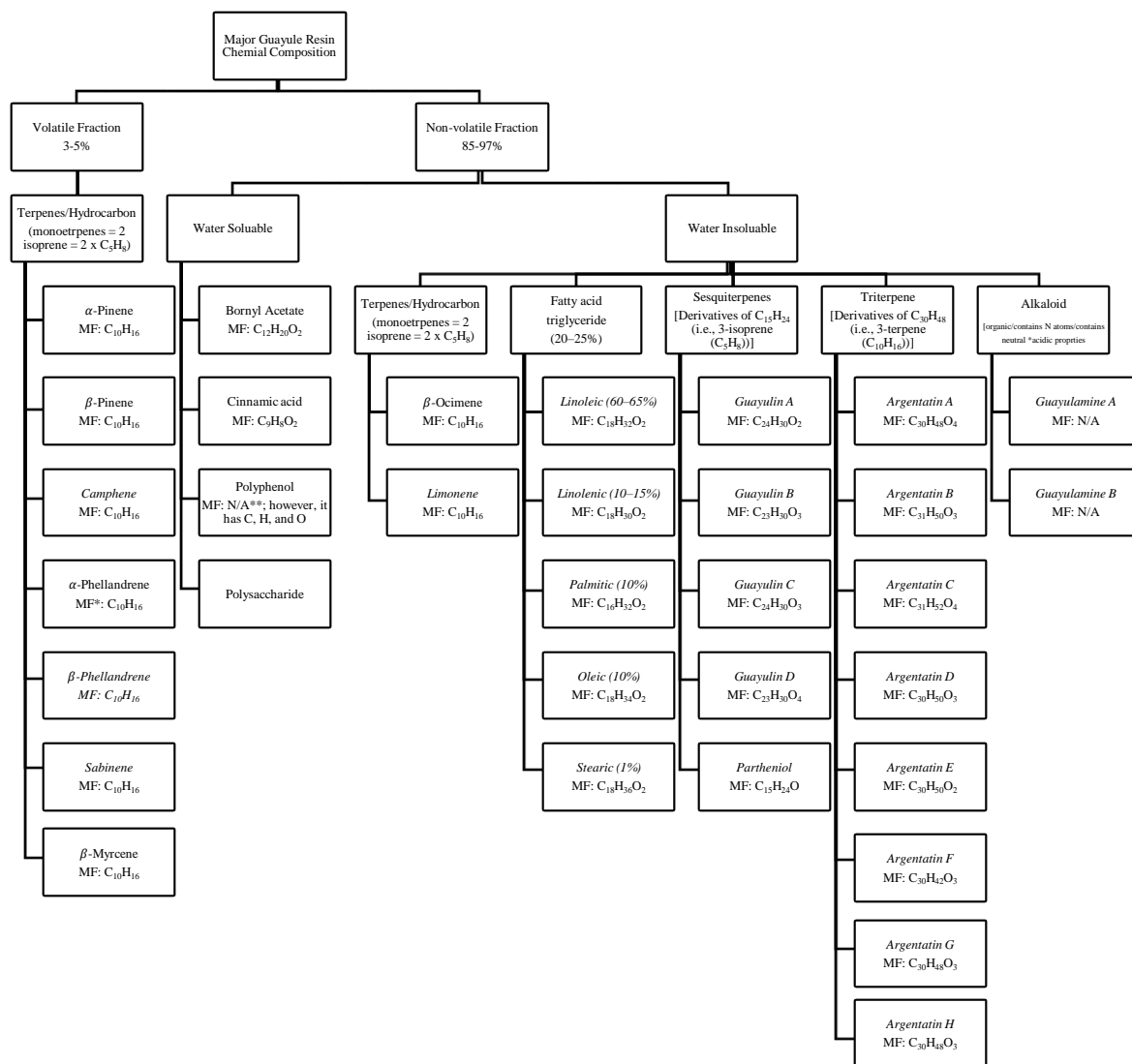
200 3. Results and Discussion

201 3.1. *Chemical analysis of guayule resin*

202 3.1.1. *Review on Chemical components*

203 Since guayule resin denotes a bio-based byproduct extracted from guayule plant with the major product (guayule
 204 natural rubber), its composition is mainly hydrocarbons, as interpreted in the following section (Nakayama, 2005).
 205 Such a composition could also be shown by the molecular formulas (MFs) of its chemical components in **Figure 1**. It
 206 is mainly composed of atoms of carbon (C), hydrogen (H), oxygen (O), and nitrogen (N). However, these atoms are

207 included in several chemical compounds. Major chemical components and their molecular formulas such as
 208 Triterpenes [Argentatin: -A ($C_{30}H_{48}O_4$), -B ($C_{31}H_{50}O_3$), -C ($C_{31}H_{52}O_4$), -D ($C_{30}H_{50}O_3$), -E ($C_{30}H_{50}O_2$), -F ($C_{30}H_{42}O_3$),
 209 -G ($C_{30}H_{48}O_3$) and -H ($C_{30}H_{48}O_3$)], Sesquiterpenes [Guayulin: -A ($C_{24}H_{30}O_2$), -B ($C_{23}H_{30}O_3$), -C ($C_{24}H_{30}O_3$) and -D
 210 ($C_{23}H_{30}O_4$), and Partheniol ($C_{15}H_{24}O$)], and many others are shown in **Figure 1** (Nakayama, 2005; NLM, 2019).
 211 Further details related to guayule resin composition could be found in “*Guayule Future Development*” (Nakayama,
 212 2005).

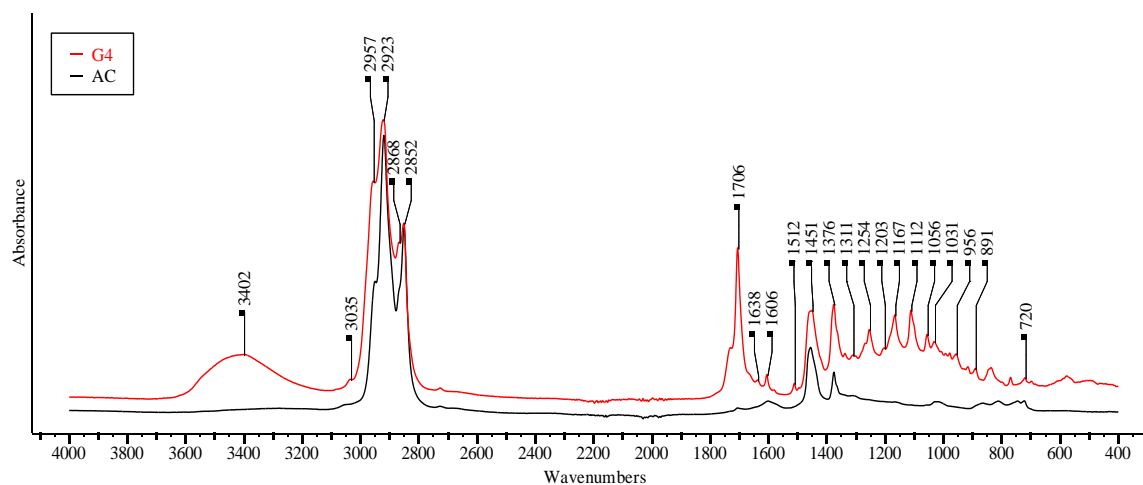


213

214 **Figure 1. Major chemical components of guayule resin. (MF, molecular formula).**215 **3.1.2. Chemical bonding**

216 FTIR spectrum of guayule resin was obtained for its chemical analysis. Guayule resin has several identical peaks
 217 similar to the base asphalt, so it is an asphalt-like material (Hemida and Abdelrahman, 2019a). Such identical peaks
 218 could be observed in **Figure 2**. It involved the four distinct peaks of symmetric and asymmetric C–H stretches in CH_2
 219 and CH_3 in the wavenumber range of $3000\text{--}2800\text{ cm}^{-1}$ (aliphatic functional groups). These four peaks were noticed at
 220 2957 cm^{-1} (CH_3 asymmetric stretching vibration), 2923 cm^{-1} (CH_2 asymmetric stretching vibration), 2868 cm^{-1} (CH_3
 221 symmetric stretching vibration), and 2852 cm^{-1} (CH_2 symmetric stretching vibration) (Nivitha et al., 2016; TFS, 2019).

222 Likewise, =C–H aromatic stretching was noticed at 3035 cm⁻¹ with a relatively much lower absorption. Other peaks
 223 were formed at 1451 and 1376 cm⁻¹ for the same functional group, indicating asymmetric and symmetric bends of
 224 CH₃, respectively (Bassler, 1981; Smith, 1998; TFS, 2019). These peaks could clarify the distinct carbon and hydrogen
 225 compositional elements of guayule resin (Costa et al., 1992; Nakayama, 2005). Other distinct peaks were observed at
 226 1706 cm⁻¹ and 1031 cm⁻¹ for C=O and S=O, respectively (Petersen, 1986). Likewise, the aromatic peaks were
 227 associated with C=C at 1606 (Nivitha et al., 2016) and 1512 cm⁻¹ (not observed in base asphalt) (Lionetto et al., 2012).
 228 Four carbon atoms in a row were observed at 720 cm⁻¹, indicating (CH₂)_n rocking absorption (TFS, 2019).



229

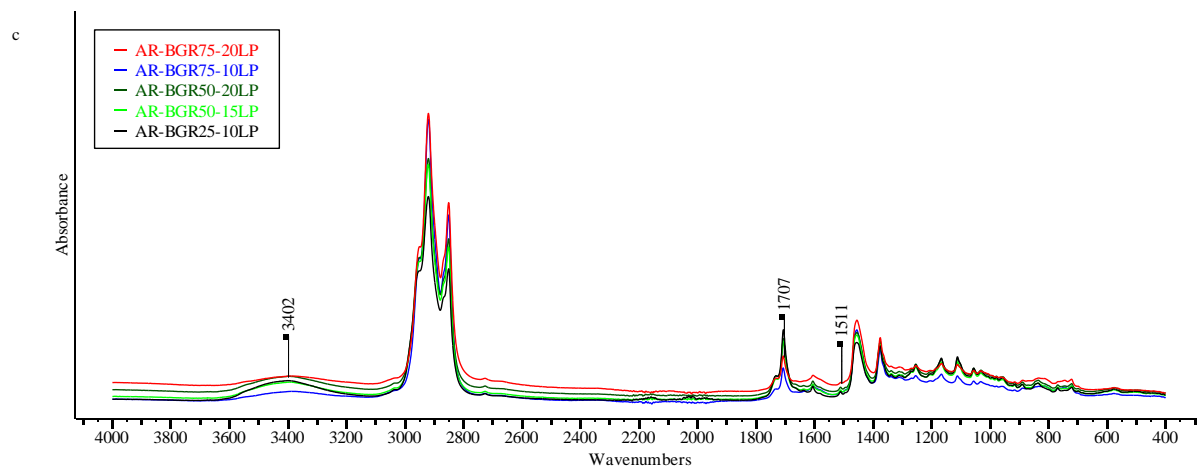
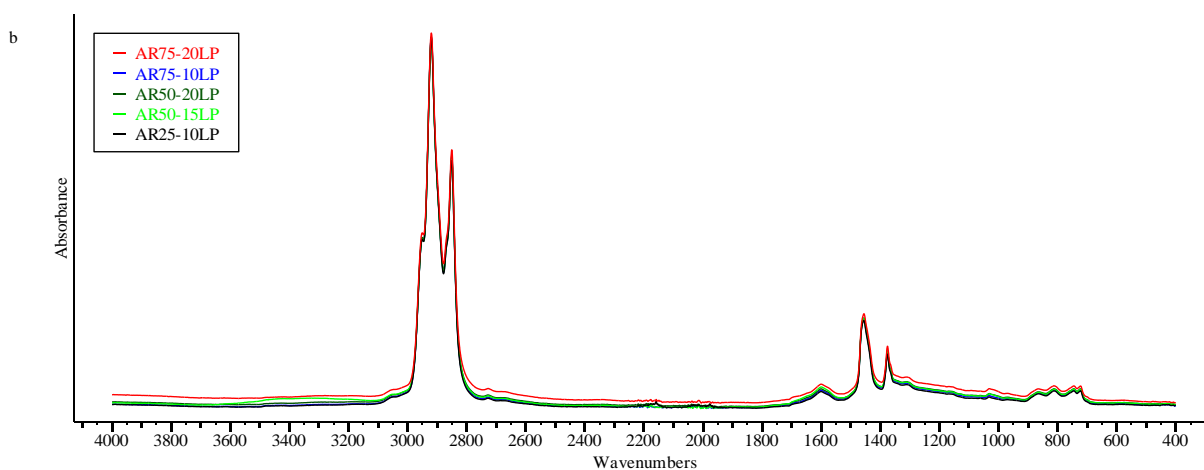
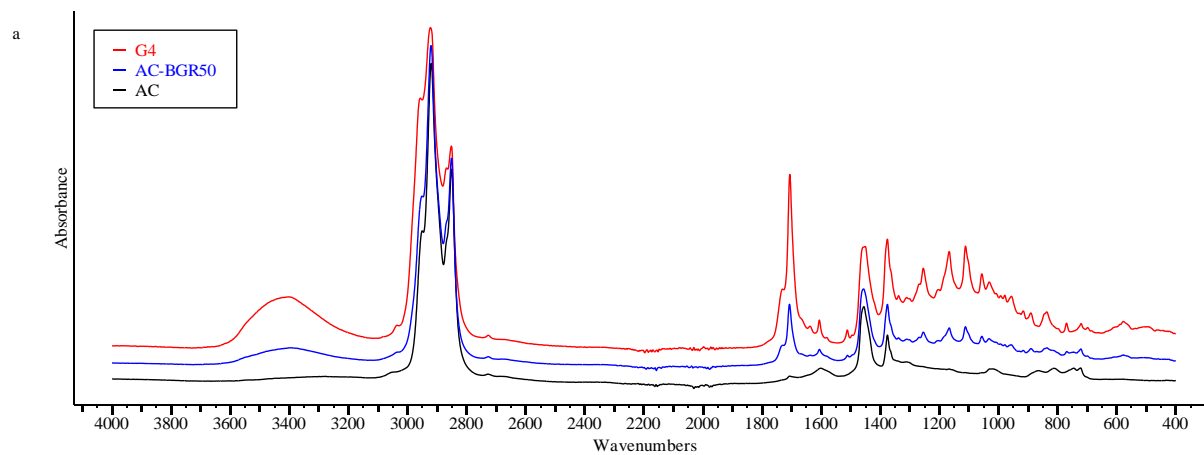
230 **Figure 2. FTIR spectra of G4 and AC (400–4000 cm⁻¹). (G4, 4-hr heat treated guayule resin; AC, base asphalt (PG64-22)).**

231 Likewise, other peaks were observed for guayule resin. Guayule resin had a peak at 3402 cm⁻¹. This peak was
 232 normally associated with broad –OH stretch (Ghobadi et al., 2018), upon which it may include alcohol. Due to
 233 hydrogen bonding, the boiling points of alcohol are much higher than the corresponding alkane with the same number
 234 of carbon atoms (TFS, 2019). The peak of NH₂ scissors stretch could be found at 1638 cm⁻¹ (Nivitha et al., 2016).
 235 Furthermore, the band at 1311 (Smith, 1998; TFS, 2019) and 1254 cm⁻¹ (TFS, 2019) was due to the stretching mode
 236 of C–O stretching of carboxylic acids. The –C–O stretching along with –OH deformation vibrations may be involved
 237 at 1203 cm⁻¹ (phenols), 1167 cm⁻¹ (tertiary alcohols), 1112 cm⁻¹ (secondary alcohols), and 1056 cm⁻¹ (primary
 238 alcohols) (TFS, 2019). Peaks from 891 to 956 cm⁻¹ may indicate the presence of OH deformation in this region
 239 (Lionetto et al., 2012).

240 Ultimately, the above discussion provides an attempt to analyze the bonds linking the guayule resin chemical
 241 elements with each other. Some peaks were emphasized with no confusion such as the aliphatic functional groups,
 242 observed in a wavenumber range of 3000–2800 cm⁻¹. However, other peaks presented potential of bond formation
 243 according to the authors' perspective, supported by literature, as interpreted by guayule resin chemical components in
 244 the previous section.

245 **3.2. Asphalt guayule interaction**

246 In order to investigate the interaction between asphalt and guayule resin, the FTIR spectrum was obtained for an
 247 asphalt guayule blend. The asphalt guayule blend was composed of half of the asphalt and the other half of the guayule
 248 resin (the so-called AC-BGR50), mixed at 3000 rpm and 190°C for 2 hr. As shown in **Figure 3a**, no new peak or peak
 249 shift occurred. However, almost all peaks included in asphalt and guayule resin were formed in the blend. Such pattern
 250 could indicate a physical interaction (no chemical interaction between asphalt and guayule resin), which was
 251 compatible with Sun et al.'s (Sun et al., 2016) finding, where the FTIR analysis of a blend of asphalt and bio-oil
 252 derived from waste cooking oil showed no chemical interaction between bio-oil and asphalt. Furthermore, Hemida
 253 and Abdelrahman (Hemida and Abdelrahman, 2020b) proved that there was no liquid phase separation between
 254 asphalt and guayule resin after lab-simulated storage. Thus, one could conclude that there was an interaction between
 255 asphalt and guayule: physical, not chemical.

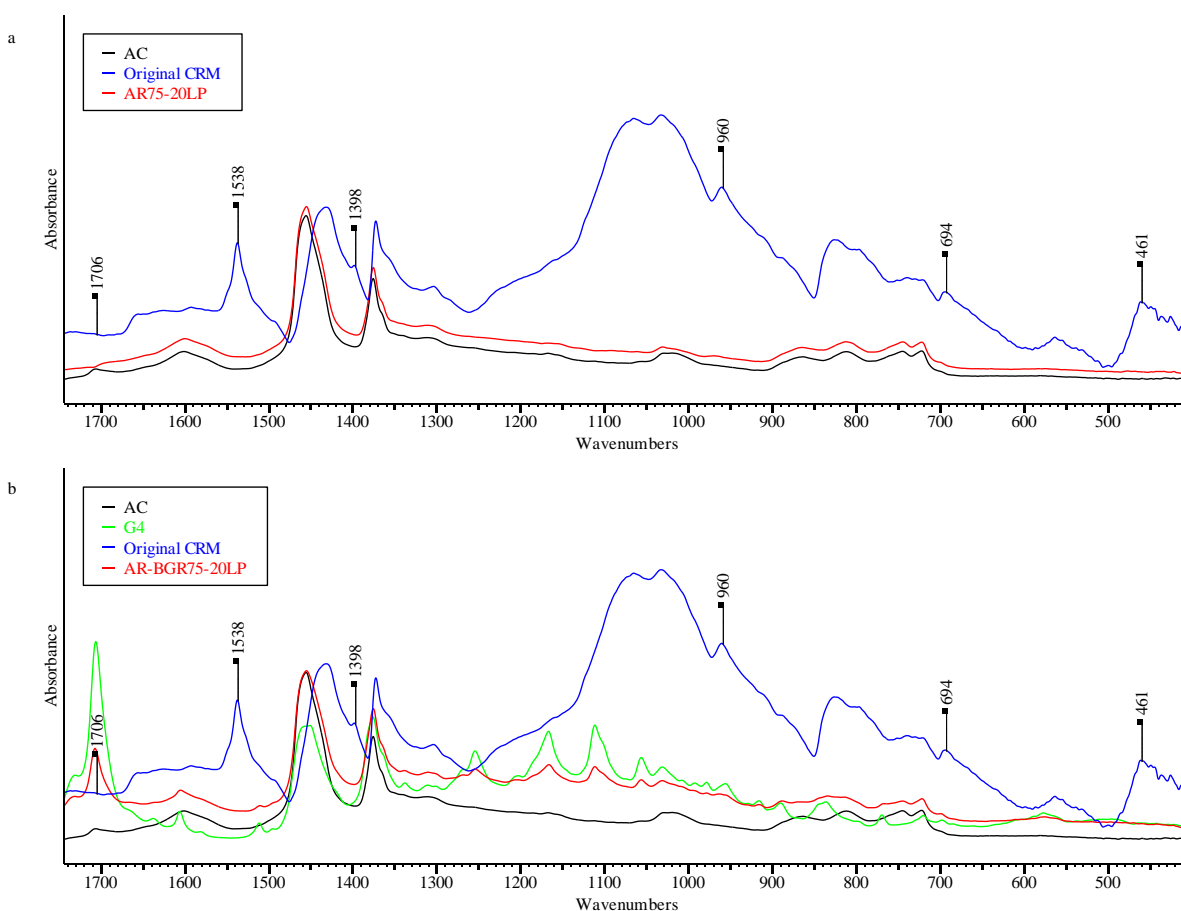


259 **Figure 3. Comparative FTIR spectra of liquid binders (400–4000 cm^{-1}):** (a) Asphalt guayule (AC-BGR), (b) asphalt rubber (AR), and (c)
 260 asphalt rubber guayule (AR-BGR). (G4, 4-hr heat treated guayule resin; AC, base asphalt (PG64-22); AC-BGR50, blend of 50% AC and
 261 50% G4; all other codes are for either asphalt-rubber-guayule bio-binders (e.g., AR-BGR25-10, 25% AR (including 10% crumb rubber
 262 modifier by wt. of AC) and 75% G4) or its corresponding asphalt rubber (i.e., the same as the bio-binder but with replacing guayule resin
 263 by extra asphalt instead, same concentration), e.g., AR25-10; LP, liquid phase/binder).

264 **3.3. Asphalt rubber guayule vs. asphalt rubber spectra**

265 The AR25-10, AR50-15, AR50-20, and AR75-10 binders had almost identical spectra (i.e., no distinct peak for
 266 one on another), indicating no changes in chemical composition regardless of material concentrations, as shown in
 267 **Figure 3b**. Like AR spectra, one may not notice distinct peak differences among corresponding AR-BGRs (**Figure**
 268 **3c**). Nevertheless, the AR-BGRs had multiple peaks, which did not appear in the corresponding AR spectra such as
 269 the very polar (-OH) group at 3402 cm^{-1} , C=O at 1707 cm^{-1} , C=C at 1511 cm^{-1} , etc. Such peaks remarkably belonged
 270 to the pure guayule resin, as discussed in Section 3.1. On the other hand, one may see the variation of AR-BGR75-20
 271 and AR75-20 spectra compared to other AR-BGRs and ARs, respectively. Such distinction will be clarified hereafter
 272 in Section 3.4.

273 For brevity, **Figure 4a** shows a portion of the AR75-20 spectrum in comparison with base asphalt and original
 274 CRM at distinct peaks. All other ARs yielded a relatively similar scenario. One can observe small peak intensities at
 275 970 and 699 cm^{-1} for AR75-20. These peaks depict a release of out-of-plane C-H bends of monoalkylated aromatics
 276 of polystyrene and trans-alkane of polybutadiene diffused from CRM to liquid asphalt (Ghavibazoo et al., 2013b;
 277 Masson et al., 2001; Ragab, 2016). Peaks at 1538 , 1398 , 461 cm^{-1} might not significantly appear in the AR75-20
 278 spectrum. However, the CRM residue chemical analysis, discussed in the next section, clarified their transfer from the
 279 CRM to the liquid binder. The Peak at 1706 cm^{-1} was also lost in AR75-20 (Ghavibazoo et al., 2013b). Such lost peak
 280 may indicate a swollen CRM particle by one of the asphalt groups, which is the C=O functional group.

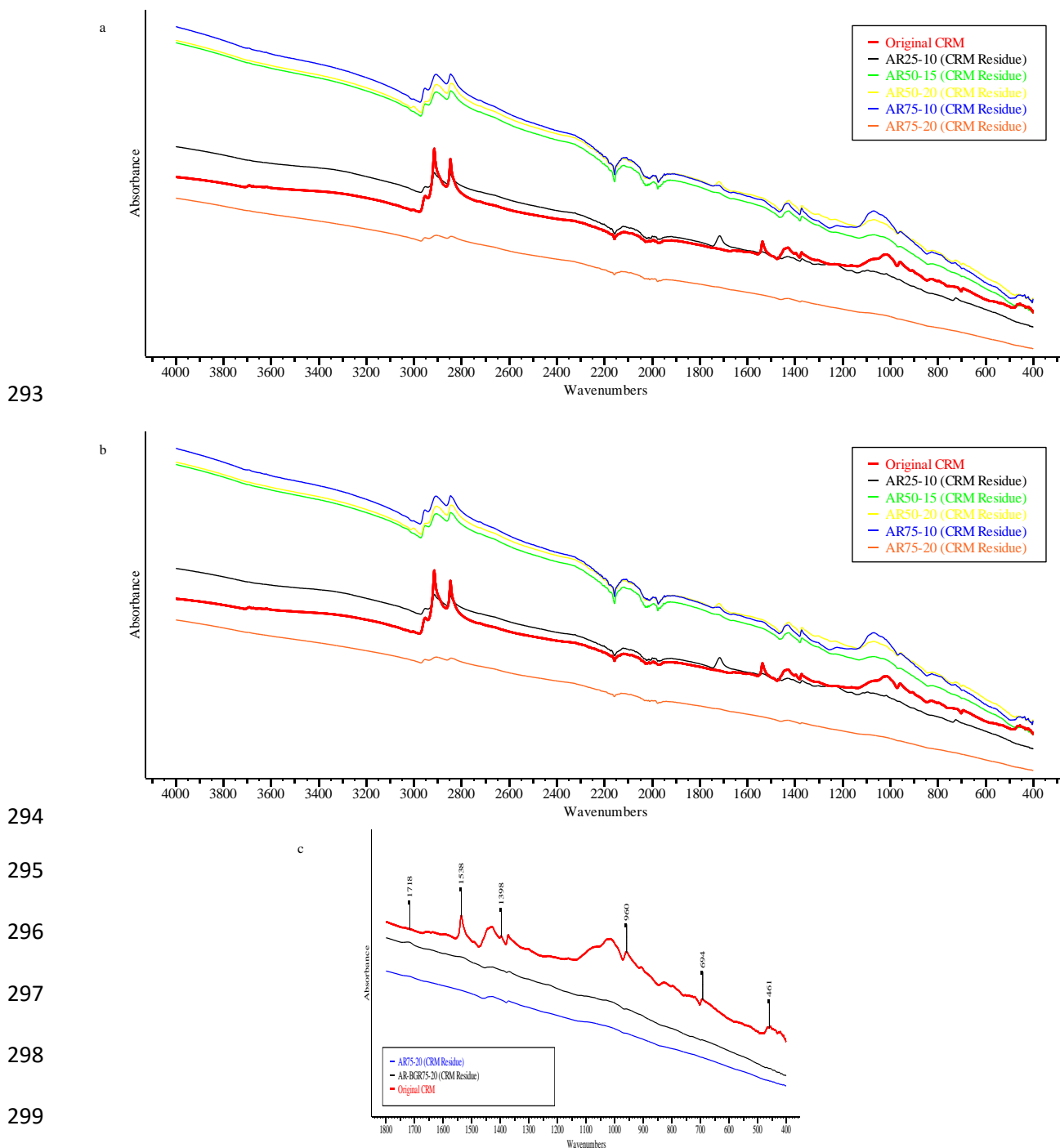


281

282 **Figure 4.** Partial FTIR spectra ($400\text{--}1750\text{ cm}^{-1}$): (a) AR75-20LP and (b) AR-BGR75-20LP, in comparison with those of original materials:
 283 AC, CRM, and G4. (AC, base asphalt (PG64-22); G4, 4-hr heat treated guayule resin; CRM, crumb rubber modifier; AR-BGR75-20, 75%
 284 asphalt rubber (including 20% CRM by wt. of AC) and 25% G4; AR75-20, the corresponding asphalt rubber by replacing the 25% G4 by
 285 extra 25% AC instead; LP, liquid phase/binder).

286 **Figure 4b** illustrates the distinct peaks investigated for AR-BGR75-20. Due to the high concentration of C=O
 287 double bond at 1706 cm^{-1} in guayule resin, a distinct peak was observed in AR-BGR75-20, but with a remarkably
 288 lower intensity. Though both guayule resin and original CRM had peak intensities around 960 cm^{-1} , related to

289 polybutadiene (Ragab, 2016; Zhang and Hu, 2015), a little-to-no peak was corresponding in AR-BGR75-20 (the same
 290 at 690 cm^{-1} , related to polystyrene). The other three peaks at 1538, 1398, and 461 cm^{-1} in the liquid AR-BGR75-20,
 291 like in its corresponding asphalt rubber (AR75-20), were not also clear. However, the CRM residue chemical analysis,
 292 in the next section, clarified their transfer from the CRM to the liquid binder.



293

294

295

296

297

298

299

300 **Figure 5. Comparative FTIR spectra of CRM residue: (a) asphalt rubber guayule, (b) asphalt rubber (400–4000 cm^{-1}), and (c) CRM residue**
 301 **of AR-BGR75-20 and AR75-20, in comparison with the original CRM (400–1800 cm^{-1}).** (CRM, crumb rubber modifier; all other codes
 302 represent either the CRM residue of asphalt-rubber-guayule bio-binders (e.g., AR-BGR25-10, 25% asphalt rubber (including 10% CRM
 303 by wt. of asphalt) and 75% 4-hr heat-treated guayule resin) or its corresponding asphalt rubber (i.e., the same as asphalt rubber guayule
 304 but with replacing guayule by extra asphalt), e.g., AR25-10).

305 **3.4. Released component verification by CRM residue Spectra**

306 FTIR was used to obtain the CRM residue spectra in order to verify the liquid binder chemical analysis. All CRM
 307 residue of AR-BGRs had similar spectra. However, a significant difference between the CRM peak intensities before
 308 and after interaction (i.e., original CRM vs. residue) was noticed, as shown in **Figure 5a**. Likewise, the same situation
 309 was associated with ARs, as shown in **Figure 5b**.

310 For all investigated CRM residue of AR-BGRs and ARs, the peaks almost disappeared at 1398 and 1538 cm^{-1} .
 311 Such lost peaks may indicate a devulcanization of S-CH_n (Cepeda-Jiménez et al., 2001; Ragab, 2016; Romero-Sánchez
 312 et al., 2005) and diffusion of C=C in carbon black (Hassan et al., 2013; Ragab, 2016), respectively. One could notice
 313 that aliphatic hydrocarbons between 3000 and 2800 cm^{-1} were affected and their intensities significantly decreased,
 314 particularly for AR-BGR75-20 and AR75-20. On the other hand, the FTIR analysis showed a new peak formed at
 315 1718 cm^{-1} (on average) in CRM residue in variant intensities. Such peak formation may indicate that the swelling of
 316 CRM was due to the absorption of light molecular weight aromatics diffused from the liquid binder into CRM residue
 317 (Ragab, 2016) (i.e., the C=O included in guayule resin and asphalt could be diffused to the CRM residue). It was
 318 evident that guayule resin had C=O bend with a remarkable intensity, compared to asphalt. Both guayule and asphalt
 319 had their original peaks around 1706 cm^{-1} ; however, the created peaks were formed around 1718 cm^{-1} .

320 In particular, CRM residue of either AR-BGR75-20 or AR75-20 remarkably lost peaks (or at least peak intensities
 321 significantly decreased) representing a high dissolution of CRM particles into the liquid binder, as verified by the
 322 TGA analysis in the next section. The CRM residue had almost no peaks at the wavenumbers of 1538, 1398, 960, 694,
 323 and 461 cm^{-1} , as shown in **Figure 5c**. Additionally, such little-to-no peaks were noticed for all other designated
 324 binders. Though a little peak attributed to AR-BGR75-20 and AR75-20 was found around 1718 cm^{-1} , this peak was
 325 found to be higher in all other AR-BGRs and ARs.

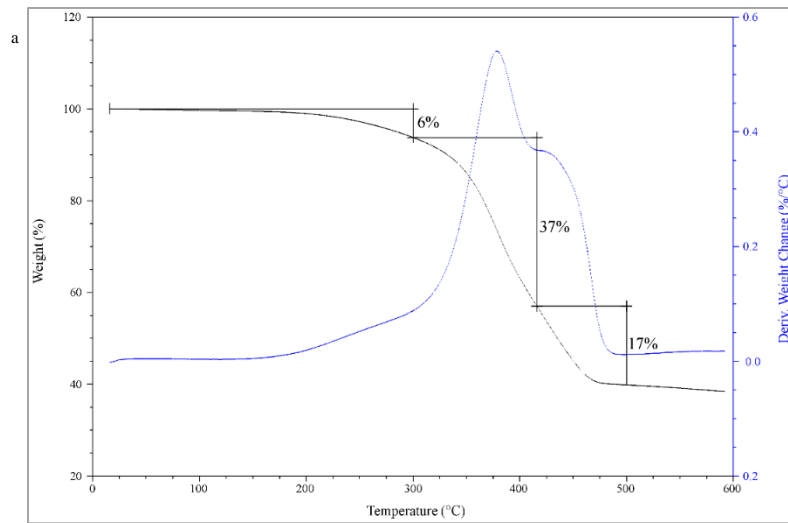
326 **3.5. TGA analysis**

327 For brevity, **Figure 6a** shows the TGA and DTG curves of original CRM explaining the CRM decomposition, as
 328 described in Section 2.2, TGA part. However, the TGA analysis was provided for original CRM and CRM extracted
 329 from all AR-BGRs.

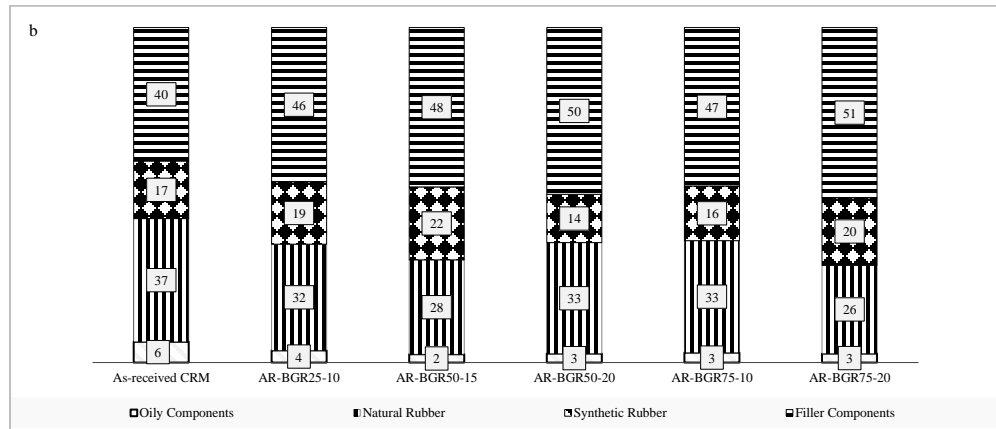
330 The distributions of CRM component proportions before and after its interaction with asphalt guayule (CRM
 331 residue) were presented. **Figure 6b** illustrates the proportional changes in CRM components extracted from AR-
 332 BGRs. One may notice that each component had close values regardless of the asphalt, rubber, and guayule
 333 concentrations, which consolidated the similarity among the FTIR spectra of the AR-BGRs.

334 **Figure 6c** illustrates the proportional changes of CRM components in the presence of the dissolved portion of
 335 CRM in the liquid binder (dissolved CRM%). A significant CRM dissolution was associated with AR-BGR75-20,
 336 which was 40%, compared to the rest of AR-BGRs. Such significant dissolution interprets the distinctive FTIR
 337 spectrum of AR-BGR75-20 compared to other bio-binders, which had relatively shorter peak intensities.

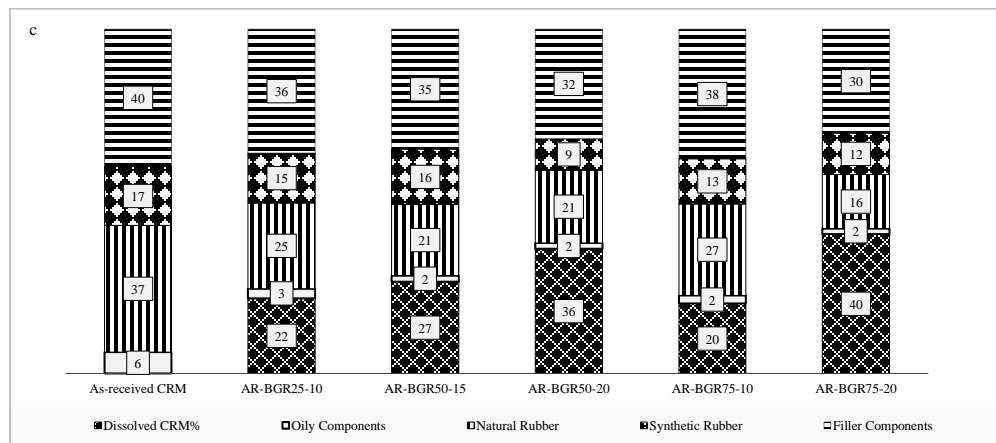
338



339



340



341 Figure 6. TGA analysis: (a) TGA and DTG curves of as-received CRM, (b) proportional changes in CRM components extracted from
 342 asphalt-rubber-guayule binders, and (c) proportional changes of CRM components in the presence of the dissolved portion of CRM for
 343 asphalt-rubber-guayule bio-binders. (CRM, crumb rubber modifier; all other codes represent either the CRM residue of asphalt-rubber-
 344 guayule bio-binders (e.g., AR-BGR25-10, 25% asphalt rubber (including 10% CRM by wt. of asphalt) and 75% 4-hr heat-treated guayule
 345 resin) or its corresponding asphalt rubber (i.e., the same as asphalt rubber guayule but with replacing guayule by extra asphalt), e.g.,
 346 AR25-10).

347 Conclusions

348 This research provided the component analysis of an innovative bio-asphalt binder made of guayule resin and
 349 crumb rubber modifier. The goal was to identify ways to create an innovative asphalt replacer for sustainable pavement
 350 using guayule resin. The study confirmed the distinct carbon and hydrogen compositional elements of guayule resin
 351 as an asphalt-like material. Asphalt and guayule have similarities in chemical composition and rheological behavior
 352 with temperature susceptibility. From analysis, no new peak or peak shift was observed for the asphalt guayule blend.
 353 This kind of blending indicated a physical interaction (i.e., no chemical interaction between asphalt and guayule).
 354 CRM was similarly released in either asphalt rubber guayule or its corresponding asphalt rubber. In other words, the
 355 guayule resin addition did not affect the CRM component dissolution through the liquid binder. However, since the
 356 base asphalt did not have the exact chemical structure of guayule resin, the rheological behavior of asphalt rubber
 357 guayule was not the same as asphalt rubber, as illustrated in **Table 1**, which was better for asphalt rubber. FTIR
 358 analysis did not show differences between varied concentrations of asphalt, rubber, and guayule, indicating no changes
 359 in chemical elements regardless of material concentrations. However, the distinct decrease in peak intensities was
 360 associated with the 75%(AR20%)+25%BGR binder, verified by the highest CRM dissolution (about 40%), illustrated
 361 by the TGA analysis. A new peak formed at 1718 cm⁻¹ in CRM residue for all investigated binders in variant
 362 intensities. Such a peak formation may indicate that the CRM swelling was caused by the diffusion of some of the
 363 liquid binder constituents (asphalt/guayule) into CRM residue. In compliance with a previous rheological study by
 364 Hemida and Abdelrahman [5], the relatively better performance of asphalt-rubber-guayule binder, which was
 365 associated with the 75%(AR20%)+25%BGR, was most likely related to such distinct chemical effect. One could
 366 conclude that such a binder of 62.5% of asphalt cement, 12.5% of crumb rubber modifier, and 25% of guayule resin
 367 has the potential to provide a binder with better high temperature performance than that of the base asphalt (PG64).
 368 On the Superpave grading system, such a binder provided a PG70 (as a whole matrix), or at the very least, a PG64 (as
 369 a liquid binder).

370 Acknowledgments

371 The authors are very grateful to the Bridgestone Corporation for creating the guayule resin in
 372 addition to providing valuable information in this regard. Likewise, special thanks go to Steven
 373 Lusher, Ph.D., for his assistance with providing the material samples and information, based on
 374 his experience with guayule.

375 References

- 376 1. AASHTO, 2013. AASHTO T315-12, Standard method of test for determining the rheological properties of asphalt binder
 377 using a Dynamic Shear Rheometer (DSR). American Association of State Highway Transportation Officials (AASHTO),
 378 Washington, D.C.
- 379 2. Bassler, G.C., 1981. Spectrometric identification of organic compounds.
- 380 3. Billiter, T., Chun, J., Davison, R., Glover, C., Bullin, J., 1997. Investigation of the curing variables of asphalt-rubber binder.
 381 *Petroleum science and technology* 15(5-6), 445-469.
- 382 4. Cepeda-Jiménez, C.M., Pastor-Blas, M.M., Ferrandiz-Gomez, T., Martín-Martínez, J., 2001. Influence of the styrene content
 383 of thermoplastic styrene-butadiene rubbers in the effectiveness of the treatment with sulfuric acid. *International journal of*
 384 *adhesion and adhesives* 21(2), 161-172.
- 385 5. Chipps, J.F., Davison, R.R., Glover, C.J., 2001. A model for oxidative aging of rubber-modified asphalts and implications to
 386 performance analysis. *Energy & Fuels* 15(3), 637-647.
- 387 6. Costa, E., Aguado, J., Ovejero, G., Cañizares, P., 1992. Conversion of guayule resin to C1-C10 hydrocarbons on zeolite
 388 based catalysts. *Fuel* 71(1), 109-113.
- 389 7. Daly, W.H., Negulescu, I., Glover, I., 2010. A comparative analysis of modified binders: original asphalts and materials
 390 extracted from existing pavements. Louisiana Transportation Research Center.
- 391 8. Deef-Allah, E., Abdelrahman, M., Hemida, A., 2020. Improving Asphalt Binder's Elasticity through Controlling the
 392 Interaction Parameters between CRM and Asphalt Binder. *Advances in Civil Engineering Materials* 9(1).
- 393 9. Diab, A., You, Z., 2017. Small and large strain rheological characterizations of polymer-and crumb rubber-modified asphalt
 394 binders. *Construction and Building Materials* 144, 168-177.
- 395 10. Ghavibazoo, A., Abdelrahman, M., 2014. Effect of Crumb Rubber Dissolution on Low-Temperature Performance and Aging
 396 of Asphalt-Rubber Binder. *Transportation Research Record* 2445(1), 47-55.

- 397 11. Ghavibazoo, A., Abdelrahman, M., Ragab, M., 2013a. Effect of Crumb Rubber Modifier Dissolution on Storage Stability of
398 Crumb Rubber–Modified Asphalt. *Transportation research record* 2370(1), 109-115.
- 399 12. Ghavibazoo, A., Abdelrahman, M., Ragab, M., 2013b. Mechanism of Crumb Rubber Modifier Dissolution into Asphalt Matrix
400 and Its Effect on Final Physical Properties of Crumb Rubber–Modified Binder. *Transportation research record* 2370(1), 92-
401 101.
- 402 13. Ghobadi, M., Gharabaghi, M., Abdollahi, H., Boroumand, Z., Moradian, M., 2018. MnFe₂O₄-graphene oxide magnetic
403 nanoparticles as a high-performance adsorbent for rare earth elements: Synthesis, isotherms, kinetics, thermodynamics and
404 desorption. *Journal of hazardous materials* 351, 308-316.
- 405 14. Glaser, R.R., Schabron, J.F., Turner, T.F., Planche, J.-P., Salmans, S.L., Loveridge, J.L., 2013. Low-temperature oxidation
406 kinetics of asphalt binders. *Transportation research record* 2370(1), 63-68.
- 407 15. Hassan, M.M., Badway, N.A., Elnaggar, M.Y., Hegazy, E.-S.A., 2013. Thermo-mechanical properties of devulcanized
408 rubber/high crystalline polypropylene blends modified by ionizing radiation. *Journal of Industrial and Engineering Chemistry*
409 19(4), 1241-1250.
- 410 16. Hemida, A., Abdelrahman, M., 2018. A Threshold to Utilize Guayule Resin as a New Binder in Flexible Pavement Industry.
411 *International Journal of Engineering Research and Applications* 8(12), 83-94.
- 412 17. Hemida, A., Abdelrahman, M., 2019a. Influence of Guayule Resin as a Bio-Based Additive on Asphalt–Rubber Binder at
413 Elevated Temperatures. *Recycling* 4(3), 38.
- 414 18. Hemida, A., Abdelrahman, M., 2019b. Review on Rheological Characterization of Bio-Oils/Bio-Binders and their
415 Applicability in the Flexible Pavement Industry. *International Journal of Civil Engineering and Technology* 10(12), 395-405.
- 416 19. Hemida, A., Abdelrahman, M., 2020a. Effect of Guayule Resin as a Bio-Based Additive on Storage Stability and Liquid Phase
417 Separation of Asphalt-Rubber Binder, The 99th Annual Meeting of the Transportation Research Board. Washington, DC.
- 418 20. Hemida, A., Abdelrahman, M., 2020b. Monitoring separation tendency of partial asphalt replacement by crumb rubber
419 modifier and guayule resin. *Construction and Building Materials* 251, 118967.
- 420 21. Huang, S.-C., Glaser, R., Turner, F., 2012. Impact of water on asphalt aging: Chemical aging kinetic study. *Transportation*
421 *research record* 2293(1), 63-72.
- 422 22. Lee, S.-J., Amirkhanian, S.N., Shatanawi, K., Kim, K.W., 2008. Short-term aging characterization of asphalt binders using
423 gel permeation chromatography and selected Superpave binder tests. *Construction and Building Materials* 22(11), 2220-2227.
- 424 23. Lionetto, F., Del Sole, R., Cannoletta, D., Vasapollo, G., Maffezzoli, A., 2012. Monitoring wood degradation during
425 weathering by cellulose crystallinity. *Materials* 5(10), 1910-1922.
- 426 24. Masson, J.F., Pelletier, L., Collins, P., 2001. Rapid FTIR method for quantification of styrene-butadiene type copolymers in
427 bitumen. *Journal of Applied Polymer Science* 79(6), 1034-1041.
- 428 25. Nakayama, F., 2005. Guayule future development. *Industrial Crops and Products* 22(1), 3-13.
- 429 26. Nivitha, M., Prasad, E., Krishnan, J., 2016. Ageing in modified bitumen using FTIR spectroscopy. *International Journal of*
430 *Pavement Engineering* 17(7), 565-577.
- 431 27. NLM, 2019. PubChem. <https://pubchem.ncbi.nlm.nih.gov/>. (Accessed Sep 13, 2019).
- 432 28. Petersen, J.C., 1986. Quantitative functional group analysis of asphalts using differential infrared spectrometry and selective
433 chemical reactions--theory and application. *Transportation Research Record*(1096).
- 434 29. Presti, D.L., 2013. Recycled tyre rubber modified bitumens for road asphalt mixtures: A literature review. *Construction and*
435 *Building Materials* 49, 863-881.
- 436 30. Ragab, M., 2016. Enhancing the Performance of Crumb Rubber Modified Asphalt through Controlling the Internal Network
437 Structure Developed. North Dakota State University.
- 438 31. Ragab, M., Abdelrahman, M., 2018. Enhancing the crumb rubber modified asphalt's storage stability through the control of
439 its internal network structure. *International Journal of Pavement Research and Technology* 11(1), 13-27.
- 440 32. Ragab, M., Abdelrahman, M., Ghavibazoo, A., 2013a. New Approach for Selecting Crumb-Rubber-Modified Asphalts for
441 Rutting and Permanent Deformation Resistance. *Advances in Civil Engineering Materials* 2(1), 360-378.
- 442 33. Ragab, M., Abdelrahman, M., Ghavibazoo, A., 2013b. Performance Enhancement of Crumb Rubber–Modified Asphalts
443 through Control of the Developed Internal Network Structure. *Transportation research record* 2371(1), 96-104.
- 444 34. Rasutis, D., Soratana, K., McMahan, C., Landis, A.E., 2015. A sustainability review of domestic rubber from the guayule
445 plant. *Industrial Crops and Products* 70, 383-394.
- 446 35. Romero-Sánchez, M.D., Pastor-Blas, M.M., Martín-Martínez, J.M., Walzak, M., 2005. Addition of ozone in the UV radiation
447 treatment of a synthetic styrene-butadiene-styrene (SBS) rubber. *International journal of adhesion and adhesives* 25(4), 358-
448 370.
- 449 36. Schloman Jr, W.W., Garrot Jr, D.J., Ray, D.T., Bennett, D.J., 1986. Seasonal effects on guayule resin composition. *Journal of*
450 *agricultural and food chemistry* 34(2), 177-179.
- 451 37. Shen, J., Amirkhanian, S., 2005. The influence of crumb rubber modifier (CRM) microstructures on the high temperature
452 properties of CRM binders. *The International Journal of Pavement Engineering* 6(4), 265-271.
- 453 38. Smith, B.C., 1998. Infrared spectral interpretation: a systematic approach. CRC press.
- 454 39. Socrates, G., 2004. Infrared and Raman characteristic group frequencies: tables and charts. John Wiley & Sons.
- 455 40. Sun, Z., Yi, J., Huang, Y., Feng, D., Guo, C., 2016. Properties of asphalt binder modified by bio-oil derived from waste
456 cooking oil. *Construction and Building Materials* 102, 496-504.
- 457 41. TFS, 2019. OMNIC Spectra Software. Thermo Fisher Scientific.

- 458 42. Thodesen, C., Shatanawi, K., Amirkhanian, S., 2009. Effect of crumb rubber characteristics on crumb rubber modified (CRM)
459 binder viscosity. *Construction and Building Materials* 23(1), 295-303.
- 460 43. Yao, H., You, Z., Li, L., Goh, S.W., Lee, C.H., Yap, Y.K., Shi, X., 2013. Rheological properties and chemical analysis of
461 nanoclay and carbon microfiber modified asphalt with Fourier transform infrared spectroscopy. *Construction and Building*
462 *Materials* 38, 327-337.
- 463 44. Zanzotto, L., Kennepohl, G.J., 1996. Development of rubber and asphalt binders by depolymerization and devulcanization of
464 scrap tires in asphalt. *Transportation Research Record* 1530(1), 51-58.
- 465 45. Zaumanis, M., Mallick, R.B., Frank, R., 2014. 100% recycled hot mix asphalt: A review and analysis. *Resources, Conservation*
466 *and Recycling* 92, 230-245.
- 467 46. Zhang, B., Xi, M., Zhang, D., Zhang, H., Zhang, B., 2009. The effect of styrene-butadiene-rubber/montmorillonite
468 modification on the characteristics and properties of asphalt. *Construction and Building Materials* 23(10), 3112-3117.
- 469 47. Zhang, F., Hu, C., 2015. The research for structural characteristics and modification mechanism of crumb rubber compound
470 modified asphalts. *Construction and Building Materials* 76, 330-342.
- 471 48. Zhang, F., Yu, J., Han, J., 2011. Effects of thermal oxidative ageing on dynamic viscosity, TG/DTG, DTA and FTIR of SBS-
472 and SBS/sulfur-modified asphalts. *Construction and Building Materials* 25(1), 129-137.

473